SPE-197101-MS

Simulation of High Water-Cut in Tight Oil Reservoirs during Cyclic Gas Injection

Chi Zhang, Ye Tian, Yizi Shen, Bowen Yao, and Yu-Shu Wu, Colorado School of Mines

This paper was prepared for presentation at the SPE Liquids-Rich Basins Conference-North America held in Odessa, Texas, USA, 7 - 8 November 2019.

Abstract

Tight oil production has increased dramatically and contributed to 61% of total US oil production in 2018. However, recovery factors for primary depletion with multistage fractured wells are low, typically less than 10%. Gas huff-n-puff emerges as a promising technique to push the recovery factor beyond 10% in tight oil reservoirs, based on laboratory studies, simulation and field pilot tests. A CO_2 huff-n-puff pilot was implemented in the Midland Basin, and data collected demonstrated significant incremental oil recovery, but with higher than expected water-cut rise.

To understand the excessive water production, a compositional model was built. Eight pseudo-components were used to match the PVT lab results of a typical oil sample in the Wolfcamp shale. A lab scale model was established in our simulator to match the results of gas huff-n-puff experiments in cores, where key parameters were identified and tuned. A half-stage model consisting of five fractures was built, where stress-dependent permeability was represented by compaction tables. Then a sensitivity analysis was conducted to understand the roles of different mechanisms behind the abnormal high water-cut phenomenon on this scale. Our simulation results have shown that initial water saturation, IFT-dependent relative permeability, reactivation of water-bearing layers, and re-opening of unpropped hydraulic fractures may all affect water-cut after gas injection. Among them, re-opening of unpropped hydraulic fractures was the most critical one.

Data from a pilot test imply substantial water production after gas injection, which may impede oil production, but the underlying mechanisms are poorly understood. A numerical model is developed to study possible mechanisms for high water-cut pilot results. This study also intends to quantify the impact of high water cut on cyclic gas injection.

Introduction

The commercial oil recovery of unconventional liquid-rich basins, such as the Permian, has been a huge success due to the combination of horizontal well and multistage hydraulic fracturing. Tight oil produced from ultralow permeability shale, sandstone, and carbonate formations contributed to approximately 61% of total U.S. crude oil production in 2018 (EIA, 2019). But smaller fracture spacings, or longer lateral length do not necessarily guarantee a long-term success. In fact, the oil recovery factor (RF) is typically lower than

10% in most unconventional oil plays and a rapid decline in production rate is often very common (Sheng, 2015). Hence IOR/EOR in tight oil reservoir has never been more important for operators.

Over the past decade, many technologies have been tested for IOR/EOR in tight oil reservoirs, among which the most promising one seems to be gas injection (hydrocarbon gas, CO_2, N2, etc.). Compared with water, gas has a much higher injectivity and could better supply reservoirs with additional energy. Gas could also lead to the swelling and viscosity reduction of oil. Besides, a reduced IFT in miscible injection often means more mobilized oil (Yang et al., 2019). Lastly, gas injection with hydrocarbon gas or CO_2 could reduce the environmental impact from gas flaring or greenhouse gas emissions (Wang et al., 2017). Gas huff-n-puff is often favored compared with flooding when reservoir permeability is lower than 1 mD, because of shorter response time and the ease of single-well operation (Sheng, 2015). Among all of the gas sources, CO_2 is an ideal solvent owing to its capability of extracting intermediate hydrocarbon components (Wang et al., 2017).

Field observations

A CO_2 huff-n-puff pilot implemented in the Wolfcamp formation of the Midland Basin suggested a significant oil rate improvement, but also an elevated water-cut with an increase up to 0.3. To the best of the author's knowledge, this phenomenon has never been reported or explained in the related literature. In order to find out the reason of high water cut occurrence during cyclic gas injection, and better to manage such excessive water production in tight oil reservoirs, the related work in the literature needs to be reviewed.

Most published studies on unconventional reservoirs focused on the incremental oil recovery after gas huff-n-puff, but paid less attention to associated water production. Hoffman and Evans (2016) reviewed several IOR/EOR pilots in the Bakken. Gas huff-n-puff pilots showed little improvement regarding oil rate and water production data was not mentioned. However, they reported a well which had neither oil or water rate increase immediately after water huff-n-puff, but almost a year later it exhibited both increased oil rate and a water-cut increase to 0.7. Hoffman (2018) summarized seven gas huff-n-puff pilots in the Eagle Ford and reported that gas injection would improve the cumulative oil production by 30%-70% in comparison to the depletion case. But no water production data were reported. An important reason is that water-cut for depletion stage is often quite stable except for an initial spike, which is largely due to the flowback to fracturing fluids (Pankaj et al. 2018). But sometimes, water cut would surge if induced fractures invaded other zones, such as the overlaying Lodgepole formation in Bakken play (Jin et al., 2017) or Bone Spring Formation in Delaware Basin (Pettit and Muirhea, 2016). Specifically, for the Wolfcamp formation in the Delaware basin, Pettit and Muirhea (2016) classified the water cut behaviors into three categories: a) High water cut, with average value as 0.8. b) Medium water cut with an average value as 0.4. c) Low to high water cut, well exhibiting water cut 0.2-0.4 at first, but then a surge to 0.9 within 6 months. Their simulation model concluded that it was the hydraulic fractures propagating from the Wolfcamp into the Bone Spring Formation, which caused the rising water-cut, and fracture height must be a critical factor contributing to excessive water production during depletion. But still little water production data is available for huff-n-puff operations in liquid-rich shale.

Water production data is more accessible in conventional, high permeable reservoirs, but the water-cut is often observed as unchanged or reduced after gas injection, especially for immiscible projects. Hsu and Brugman (1986) reported an immiscible CO_2 huff-n-puff pilot by Texaco in Paradis Field, Louisana. The pre-injection water cut was 0.9, and the average water-cuts for first and second cycle were almost unchanged. Denoyelle and Lemonnier (1987) reported a stripper well case in a shallow sandstone reservoir with permeability ranging from 5~20 mD and in-situ oil viscosity as 2.68 cP. Though not explicitly mentioned, the project should be immiscible as a black oil simulator was used. Before CO_2 injection, the well produced at 2 bbl/day with water-cut as 0.9. After CO_2 injection, water-cut first decreased, and then bounced back to 0.9. Haskin and Alston (1989) evaluated 28 immiscible CO_2 huff-n-puff projects in Miocene reservoirs and

found that water rates would generally decrease with increased oil rate after injection, and finally water-cut would return to the pre-injection value. Monger and Coma (1988) summarized nine successful pilots in south Louisiana oil-bearing sands. Eight of the wells experienced water-cut reduction after CO_2 injection. Only one well, Well J, experienced a water-cut surge from 0.30 to 0.67 after injection. Unlike the other eight wells, this well was apparently injecting above the MMP (Minimum Miscibility Pressure). Hence achieving miscibility might or not be a vital factor for water-cut surge.

Monger et al. (1991) reported an immiscible CO_2 huff-n-puff in the Appalachian Basin in Eastern Kentucky. 65 wells were tested in a fractured reservoir with average permeability as 10 mD. The author compared water-cut data before and after CO_2 injection and proposed that water was pushed away by injected CO_2, leading to a reduced water-cut. For the viscous oil, there was even a patented technology, called the Anti-Water Coning Technology (AWACT), which involves injecting immiscible gas into a watered-out well to suppress water conning (Luhning et al., 1990). AWACT succeeded in 40 wells in South Jenner oil Field with the in-situ viscosity as 97 cP (Lai and Wardlaw, 1999). The reduced water-cut and improved oil recovery were attributed to the trapped gas which lowered the relative permeability to water and redirected the water influx. Mohammed-Singh et al (2000) reviewed sixteen CO_2 huff-n-puff projects in the Forest Reserve oilfield of Trinidad and Tobago. Projects were successful in reservoirs with in-situ oil viscosities from 0.5 to 3000 cP and permeabilities ranging from 10 to 2500 mD. They concluded that CO_2 injection could reduce the relative permeability to water phase due to trapped gas saturation and oil swelling. Hence redistribution of fluid saturation and its resulted relative permeability alteration due to injection might be also influential factors.

Simpson (1988) reported two immiscible CO_2 huff-n-puff tests in a bottom-water reservoir with water-cut between 0.98 and 0.99, caused by water coning. Though both tests witnessed incremental oil production, the water-cut responses were very different. For Well 271, the water cut was as low as 0.002 once the puff started. Then within five days, the water cut increased to 0.57; but it remained between 0.7 and 0.8 for almost two months. Finally, it went back to the pre-test value as 0.99 in 100 days. For Well 272, once the puff started, the water-cut was continuously decreasing from 1 to 0.78, and it rose again back to 0.92. Then the well was shut-in again for two months, and water cut again reduced to 0.76, but gradually returned to the pre-test value as 0.99 in 50 days. Well 271 was shut-in for 51 days in contrast to 28 days of Well 272. Moreover, Well 271 received 18% more CO_2 than Well 272 within the 5-day injection time. Operation parameters such as shut-in time and injected gas volume may contribute to the different water-cut responses.

Laboratory studies

Many lab-scale investigations of CO_2 injection have been performed on low-permeability cores, but most of them focused on the improved oil recovery. Very few of them contemplated initial water saturation (Tovar et al., 2014; Jin et al., 2017; Song and Yang, 2017; Li et al., 2018) and let alone the production of water. For example, Tovar et al. (2014) investigated CO_2 huff-n-puff in preserved shale samples of nD permeability with packed glass beads simulating fractures. Their work confirmed the incremental RF but observed no water production even with initial water saturation estimated as 0.3. Li et al. (2018) investigated the effect of water on CO_2 huff-n-puff performance and found that RF would decrease 45% with an initial Sw as 0.4 in contrast to cores without water. Water-cut though not explicitly plotted was increasing with time.

In highly permeable rocks, water related data is still very limited. Darvish et al. (2006) investigated the efficiency of immiscible CO_2 injection into fractured cores with permeability of 4 mD. CO_2 was injected to displace the residual oil in a water-flooded core. The results indicated that the water production rate was around ten times higher than oil rate at first, and it decreased to zero after several days. The author concluded that the high-water cut was the result of high initial water saturation in the core. Torabi and Asghari (2010) examined the performance and efficiency of cyclic CO_2 injection in light-oil fractured porous media. Two Berea cores were tested as matrix with permeability of 100 and 1000 mD, respectively. The cylindrical

core was held in a steel cell with 0.5 cm annular spacing to simulate a matrix and surrounding fracture in this set-up. The results suggested that connate water existence would favor RF during immiscible CO_2 huff and puff processes, but there was no obvious difference in RF for miscible condition. Abedini and Torabi (2014) investigated CO_2 huff-and-puff in cores with permeability around 70 mD and connate water saturation ranging from 0.443 to 0.459. Their experimental results indicated that no water production was found after CO_2 injection even for cases above MMP.

In summary, the initial water-cut spike during depletion of liquid-rich unconventional reservoirs is largely due to the flowback of fracturing fluids. Fracture propagation into adjacent water layers is a possible reason for water-cut growth after flowback. For conventional reservoirs, gas injection rarely results in water-cut increase, even for watered-out wells except one case when injection was under miscible condition. Fluid saturation redistribution and a further shifted relative permeability curve might also be important factors. The injection scheme, such as shut-in time, and injected volume may also affect the behavior of the water-cut. Experimental studies of gas huff-n-puff in cores have shown contradicting roles of initial water saturation on oil RF, but initial water saturation is a decisive factor worth exploring during gas huff-n-puff. We hence investigated the above-mentioned relevant factors with a compositional model, whose key inputs including pseudo-components and corresponding fluid properties, relative permeability curves were all specified based on the related laboratory studies. The established workflow is not only of great importance for engineers to understand the reason of high water cut during cyclic gas injection, but also of great use to manage excessive water production for gas EOR in tight oil reservoirs.

Matching experiment results

The results from PVT data and core experiments were matched first to provide critical inputs for the reservoir-scale model.

PVT model

The composition of a typical oil sample from Wolfcamp shale has been analyzed up to C_{36+} in the laboratory. In this study, components were lumped into eight pseudo-components, i.e., C_1, CO_2, N_2-C_2, C_3, C_{4-6}, C_{7-15}, C_{16-24}, and C_{25+}. Their properties were tuned to match the various experiment results, including constant composition expansion, differential liberation, and swelling test. Since CH_4 will also be used as injectant in our future work, it was deliberately not lumped together with CO_2. C_3 was also listed as an individual pseudo-component to represent the improved recovery of natural gas liquids (NGL). The PVT model utilized the Peng-Robinson (PR) equation of state (EOS) and the calculated curves after regression in WinProp matched the original experimental data well, as shown in Figure 1.

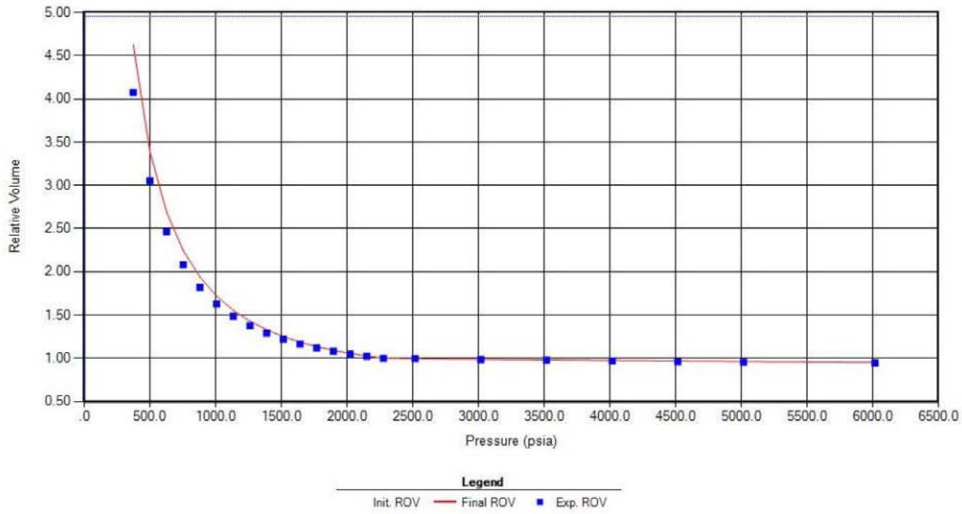

(a) Constant composition expansion

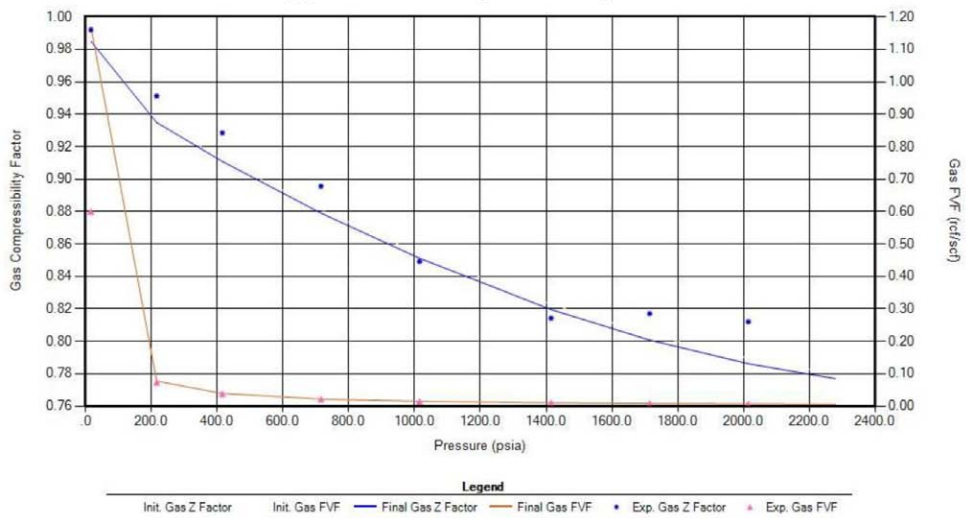

(b) Differential liberation test

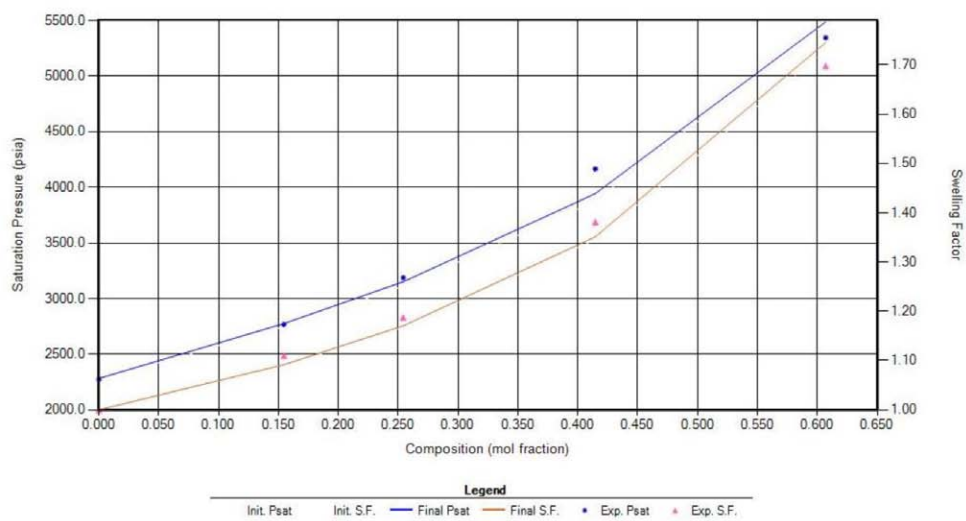

(c) Swelling test

Figure 1—Matching the experimental results with the PVT model

After tuning, the composition and thermodynamic properties for each component are summarized in Table 1. PR EOS was used to calculate the oil properties at the reservoir temperature of 170 °F, and estimated the saturation pressure as 2,263.7 psi, oil gravity as 43 °API, formation volume factor as 1.38 rb/STB and GOR as 780 SCF/STB. The minimum miscibility pressure (MMP) between the reservoir oil and injected CO_2 was estimated as 2,020.4 psi.

Table 1—Properties of the pseudo-components of a typical oil sample in Wolfcamp Shale

Pseudo-component	Mole fraction	Pc, atm	Tc, K	Vc, L/mol	Acentric Factor	MW, g/mol
CO_2	0.0048	72.80	304.2	0.0940	0.2250	44.0
CH_4	0.3517	45.40	190.6	0.0990	0.0080	16.0
N_2-C_2	0.0972	48.06	301.2	0.1464	0.0966	30.0
C_3	0.0801	41.90	369.8	0.2030	0.1520	44.1
$C_{4\text{-}6}$	0.1173	34.84	457.4	0.2919	0.2260	69.2
$C_{7\text{-}15}$	0.2400	25.42	616.6	0.5096	0.4277	138.6
$C_{16\text{-}24}$	0.0592	14.95	828.1	0.9833	0.7949	265.4
25+	0.0496	15.00	987.8	1.4830	1.1223	359.6

Lab-scale huff-n-puff model

An experiment was designed specially to conduct gas huff-n-puff tests in a composite core, consisting of a low permeability rock and a high permeability rock, as shown in Figure 2. The low permeability rock had a permeability of 0.11 mD, equivalent to the effective permeability of Wolfcamp matrix and natural fractures. The high permeability rock with a permeability of 2,200 mD represented the propped hydraulic fracture. The core holder was maintained at reservoir temperature of 170 °F through a run. The initial oil saturation was estimated at 0.5 in the low permeability rock and 0.0 in the high permeability rock. The system was initially at 4,000 psi and then depleted to 600 psi. Gas was then injected through top rock and pressurized the system to 4,000 psi. The system was closed to simulate soaking processes and was depleted to 600 psi again. The produced oil and water were collected and measured during the production period. All the experimental data presented here was provided by our industry partner.

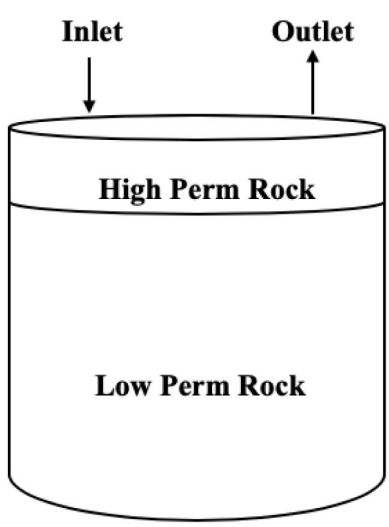

Figure 2—Schematic of gas huff-n-puff set-up with composite cores

A simulation model was built to match the results of lab-scale experiments. There were 10 grids in radial direction and 6 grids in axial direction in the cylindrical model, as shown in Figure 3. The PVT model established earlier was used in this lab-scale model.

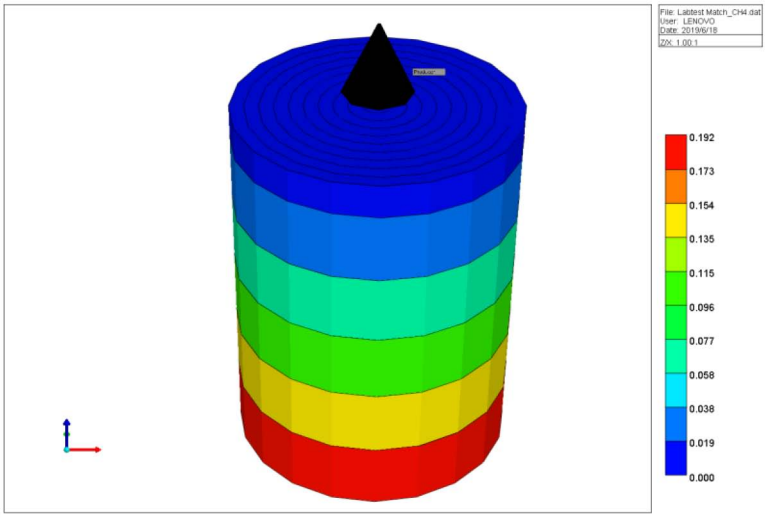

Figure 3—Simulation model for Lab-scale gas huff-n-puff

History matching of the experimental results were then completed. Since the BHP (bottom hole pressure) was set as well constrain during the whole simulation process, its values were the same as the history data. Relative permeability curves of tight rock representing matrix were tuned primarily to match the cumulative oil and water production as shown in Figure 4. Though the water-oil ratio is lower than the value observed in the field, the water production was not zero unlike many previous huff-n-puff experiments in tight cores.

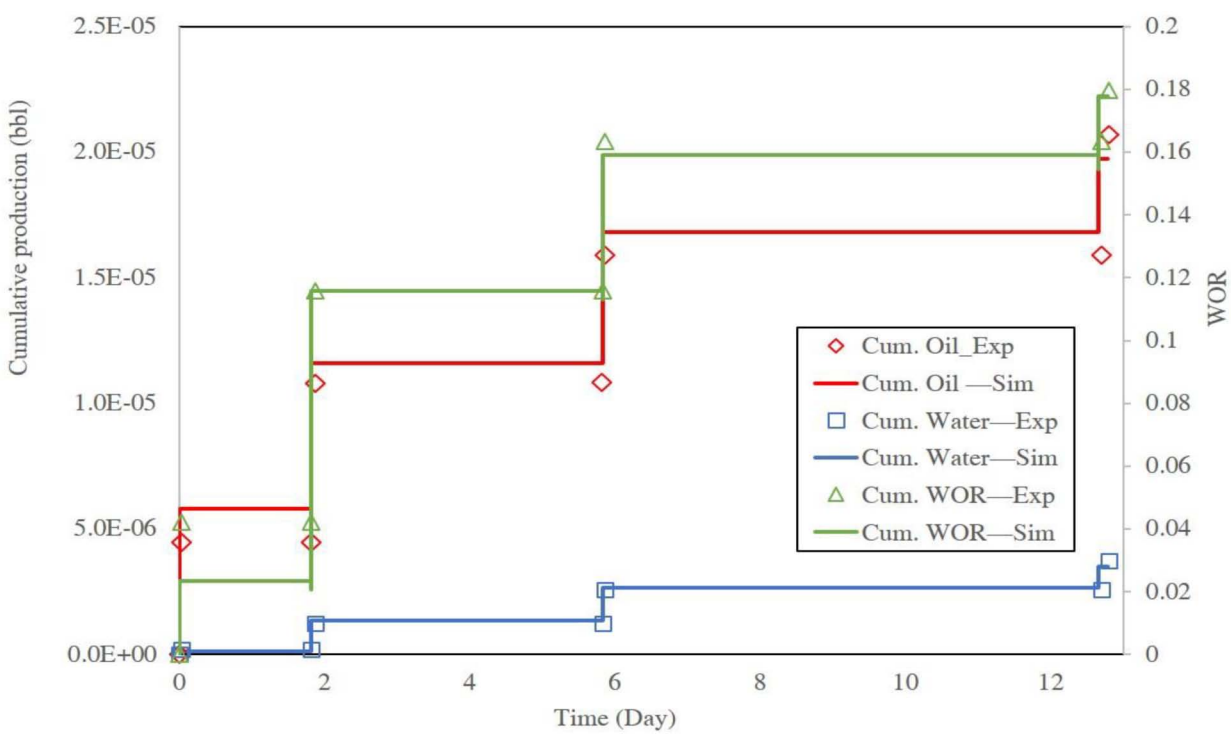

Figure 4—Matching the experiment results

And the relative permeability curves for high permeability rock representing fractures were generated by assuming a minimal residual saturation for all phases. The final relative permeability curves that led to the best match are shown in Figure 5 and Figure 6. Matrix rock compressibility was also found decisive in the matching process and a final value of 5×10^{-6} psi^{-1} was found to provide the best match. Please note that the original experiment used CH_4 as the injected gas, but the water-oil relative permeability curves should be reliable after matching. And it was assumed that gas-liquid curve for CH_4 and CO_2 was the same.

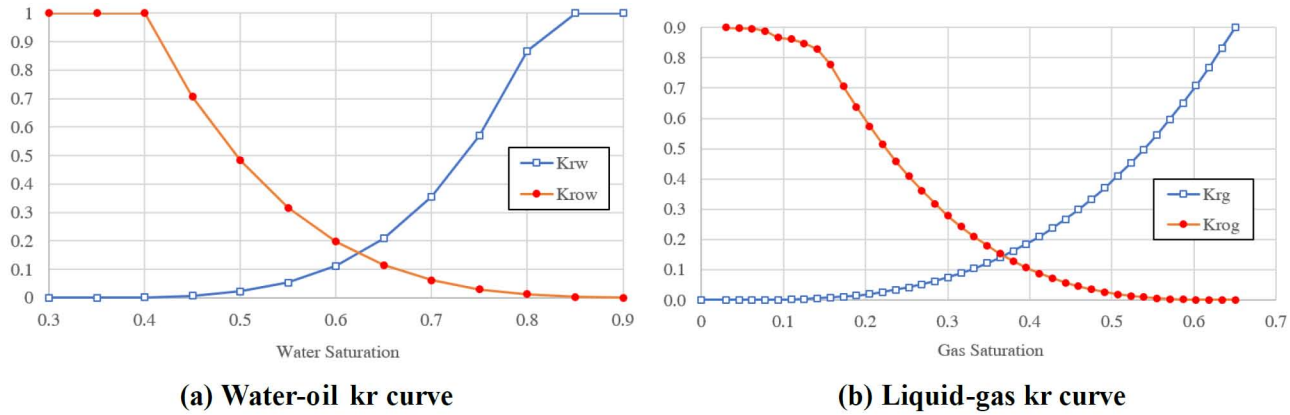

(a) Water-oil kr curve (b) Liquid-gas kr curve

Figure 5—Matrix relative permeability curves obtained after history match

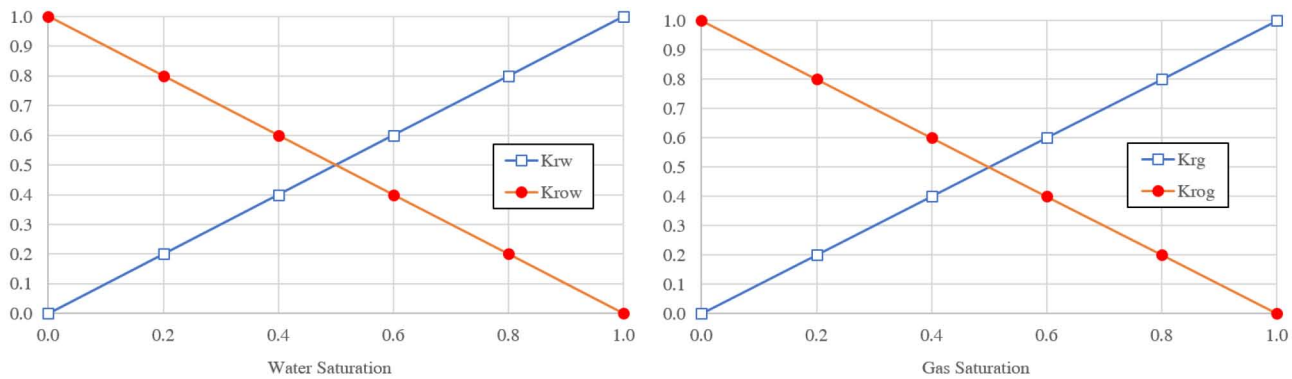

(a) Water-oil kr curve (b) Liquid-gas kr curve

Figure 6—Fracture relative permeability curves

Set-up of the base case

A typical horizontal producer in this region has a perforated lateral length of 10,000 ft with 100 fracturing stages. There are five perforation clusters in each stage, which are assumed identical to each other and uniformly distributed over the lateral as shown in Figure 7. Propped and unpropped hydraulic fracture, enhanced permeability region, and natural fracture and matrix were entirely taken into consideration in the model, as shown in Figure 8. The dual permeability model is used to capture natural fracture networks. Within a hydraulic fracture, it is assumed that the fracture tip region is unpropped, therefore has a smaller conductivity (blue region). The hydraulic fracture half-length is 390 ft and propped length (red and yellow region) is 147 ft.

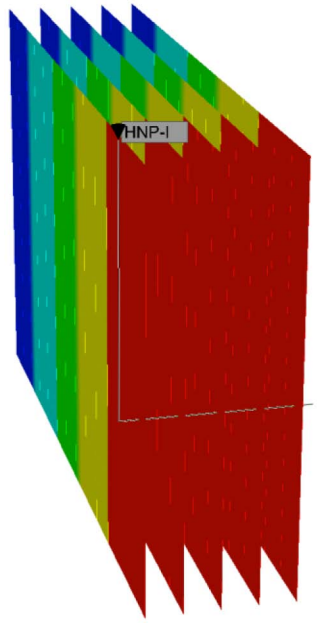

Figure 7—Schematic of the conceptual reservoir model

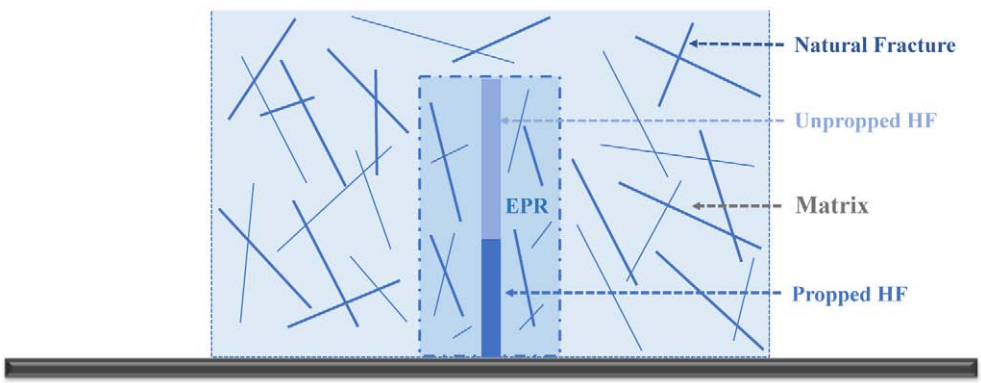

Figure 8—Half of a symmetric element conceptual model (top-down view)

The width of the model in I direction is 100 ft to cover a single fracturing stage. Since the distance between two parallel horizontal wells in J direction is set to be 880 ft, by assuming they are identical, and a closed flow boundary can then be established by symmetry. Therefore, the whole stage can be simplified with a half-stage model with size as 440 ft in J direction. In K direction, there is no symmetry hence the entire formation is modelled with all 15 layers. The simplification using symmetry was commonly used in other work (Brown et al., 2011; Tian et al., 2019). Table 2 summarizes the geometry of the half-stage model with five planar fractures.

Table 2—Geometry of the base case for reservoir simulation

Well geometry		Model dimension	
Perforated lateral length, ft	10000	X, ft	100
Stage number	100	Y, ft	440
Clusters per stage	5	Z, ft	236
Cluster spacing, ft	20	Fracture half-length, ft	390

For the primary mesh, there are 35 grid blocks in the I-direction, 15 grid blocks in the J direction, and 15 grid blocks in the K direction. Then the hydraulic fractures are created with template and refined grids are used near the fracture which makes the total grid block number as 14,625. The grid system of the conceptual model after refinement is shown in Figure 9.

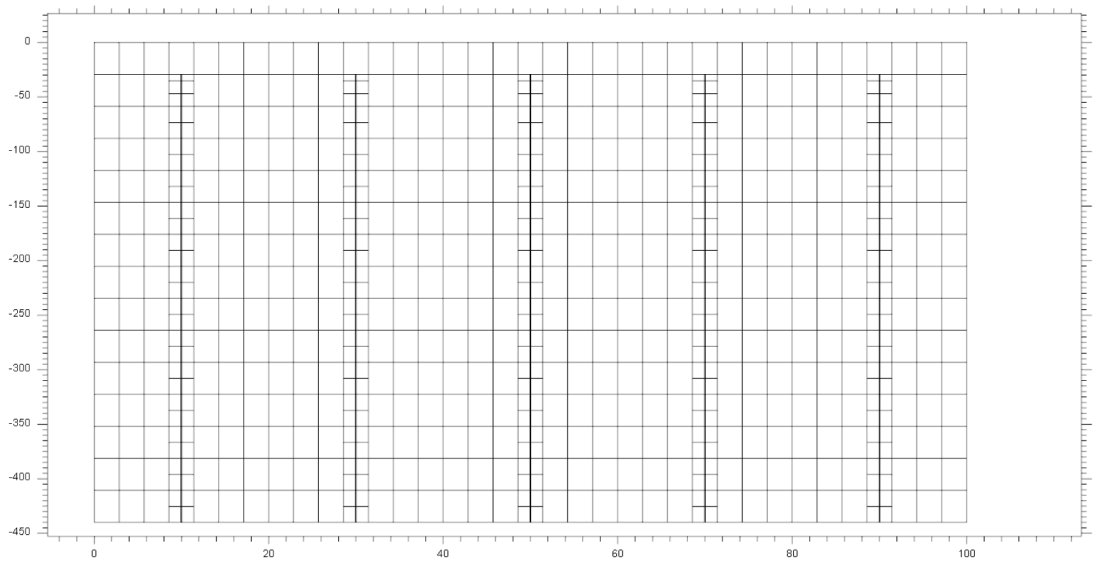

Figure 9—The grid system in the I-J plane for the base case

For the natural fracture mesh, it is assumed that porosity is constant as 0.0001 and horizontal permeability as 0.025 mD. For the matrix grid block, it is assumed that rock properties including porosity, horizontal permeability, and initial water saturation only vary vertically and within each layer they are all homogeneous. The matrix properties of different layers are summarized in Table 3. For both matrix and fracture, vertical permeability is assumed to be one tenth of horizontal permeability. The natural fracture spacing is 50 ft in I, J direction and 0 ft in in K direction.

Table 3—Rock properties of the matrix grid at different layers

Layer	Thickness, ft	Porosity	Permeability, mD	Initial water saturation
1	10	0.0661	2.046E-04	0.57
2	30	0.0581	1.271E-04	0.68
3	24	0.1037	1.101E-03	0.36
4	18	0.0713	2.720E-04	0.36
5	13	0.0617	1.591E-04	0.65
6	17	0.0598	1.409E-04	0.70
7	13	0.0677	2.240E-04	0.59
8	17	0.0590	1.346E-04	0.66
9	15	0.0499	7.171E-05	0.84
10	13	0.0502	7.371E-05	0.94
11	12	0.0362	2.171E-05	1.00
12	15	0.0338	1.686E-05	0.81
13	15	0.0882	6.020E-04	0.70
14	10	0.0439	4.457E-05	0.63
15	14	0.0763	3.509E-04	0.53

Since the hydraulic fracture (HF) is modeled explicitly by local refined grids, and the grid width w_{grid} containing HF as 0.1 ft is much larger than the actual width of HF, w_{HF} as 0.001 ft. The grid effective permeability k_{HFeff} is scaled accordingly to maintain the same fracture conductivity as specified (CMG, 2018).

$$k_{HFeff} = \frac{k_{HF} w_{HF}}{w_{grid}} \quad \text{Eq. 1}$$

For example, the grid block effective permeability for the propped HF is 50 mD, which is the propped HF's conductivity (5 mD·ft) divided by the grid width (0.1 ft). The stress-dependency of fracture permeability is modelled by the usage of a compaction table. The unpropped HF and natural fracture (NF) are assumed to follow the same trend, while propped HF should follow a different curve with weaker dependency on stress and higher remaining permeability as shown in Figure 10.

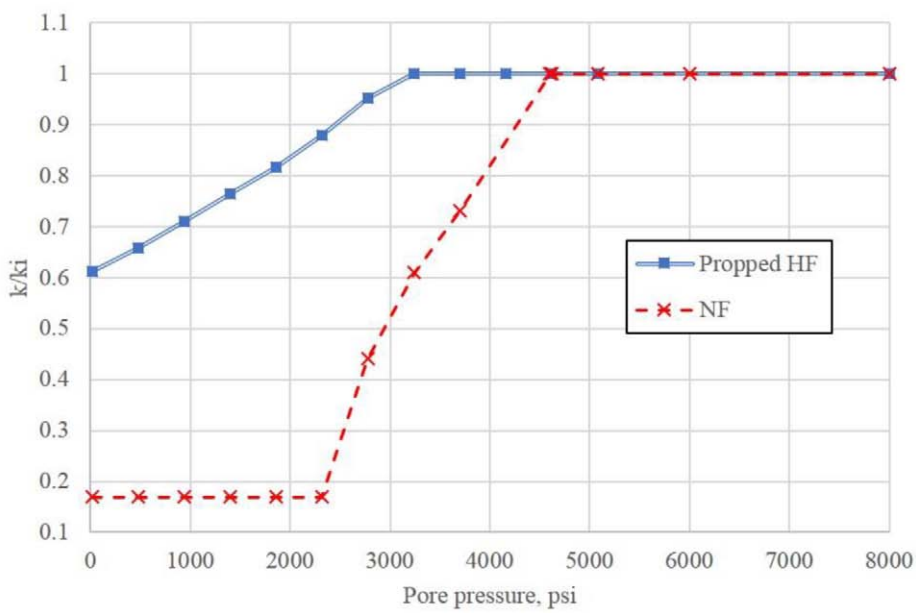

Figure 10—The stress-dependent permeability correlation in the model

In order to simulate the water-cut spike caused by flowback, water was first injected with total volume as 2,320 STB to match a typical stimulation design for the half-stage model in this region. The well was first depleted for four years with a maximum oil rate as 10 STB and a minimum BHP set as 1,200 psi. Then the well was injected with a maximum CO_2 rate as 6,000 SCF/day and maximum BHP as 7,000 psi for 50 days. Shut-in time was set as 10 days. In the puff stage, the well was set to produce with a maximum oil rate as 10 STB and minimum BHP as 1,200 psi for 300 days. It is worth mentioning that the "stage" in our model is a half-stage, hence a factor of 200 should be used for scaling rates to a well with 100 full stages.

Results and discussions

A sensitivity study was carried out to quantify the impacts of high water cut. The goal of this paper is to provide insights into key parameters controlling the high water cut after a CO_2 huff-n-puff process in the Wolfcamp formation.

Huff-n-puff v.s. depletion

The base model was established with six CO_2 huff-n-puff cycles simulated. A case with only depletion was also run as shown in Figure 11. The recovery factor for huff-n-puff case was 11.46%, which was 1.48 times

of the RF of depletion as 7.74%. The improvement factor as 1.48 matched the field observations in the literature (Wang et al., 2017; Hoffman, 2018).

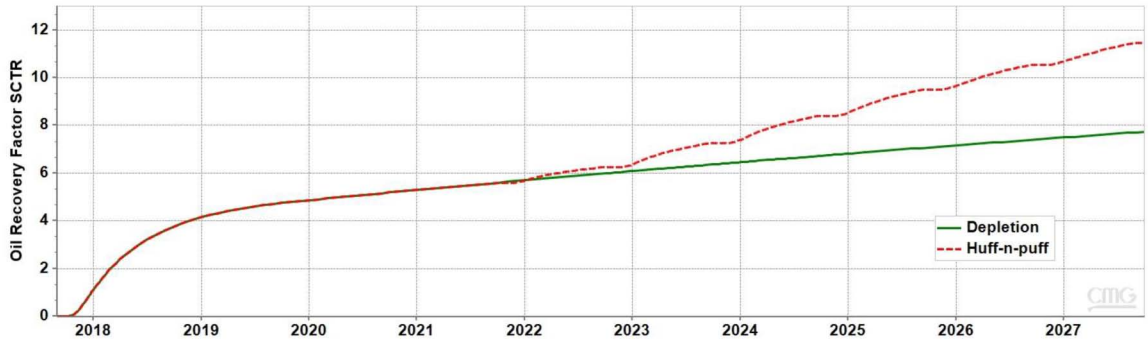

Figure 11—Comparison of huff-n-puff and depletion oil recovery factor

Table 4 shows the component RF of C_3. After gas injection, less C_3 was recovered from oil phase, but more significantly amount of C_3 increase was found in the produced gas, demonstrating increased yield of NGL and the enrichment of the produced gas due to vaporizing effect. And the component RF of C_3 was slightly higher than that of oil due to the compositional nature of the gas huff-n-puff.

Table 4—Component Recovery Factor of C_3

	Produced C3 in Oil, mol	Produced C3 in Gas, mol	Original in place, mol	RF
Depletion	89991	279217	369208	7.73%
Huff-n-puff	87333	482661	569994	11.93%

With respect to water-cut, it reached a peak at 1.0 due to flowback, then it fell and remained almost constant as 0.38 which represented a typical water-cut behavior during depletion. For huff-n-puff, the water cut would start at a very low value i.e. 0 as only CO_2 was being produced when the well was first opened. It then would reach a peak as 0.43 around 10 days and fell to value as 0.36. Finally, it would bounce back to a plateau as 0.44 and remain constant for the rest of puff stage. With more cycles, the peak would gradually increase, and the plateau value would decrease as shown in Figure 12.

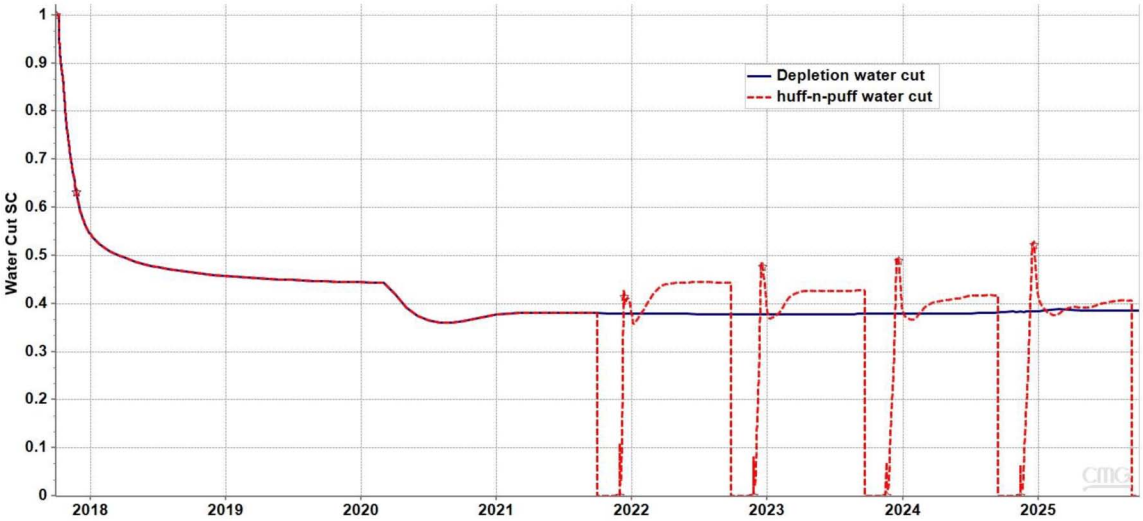

Figure 12—Comparison of huff-n-puff and depletion water-cut

Interestingly, the simulated water-cut somehow resembles the water-cut response of Well 271 with CO_2 huff-n-puff in a conventional reservoir (Simpson, 1988) as shown in Figure 13. But it is different from what was observed in the CO_2 pilot for Wolfcamp formation. The observation from the unconventional play in the CO_2 pilot for Wolfcamp formation of Midland shows that the water cut will increase 0.3 from depletion basis. It will slightly decrease at early stage for each cycle but remain at a level higher than depletion. Hence, we hereinafter explore several possible reasons behind abnormal water-cut response.

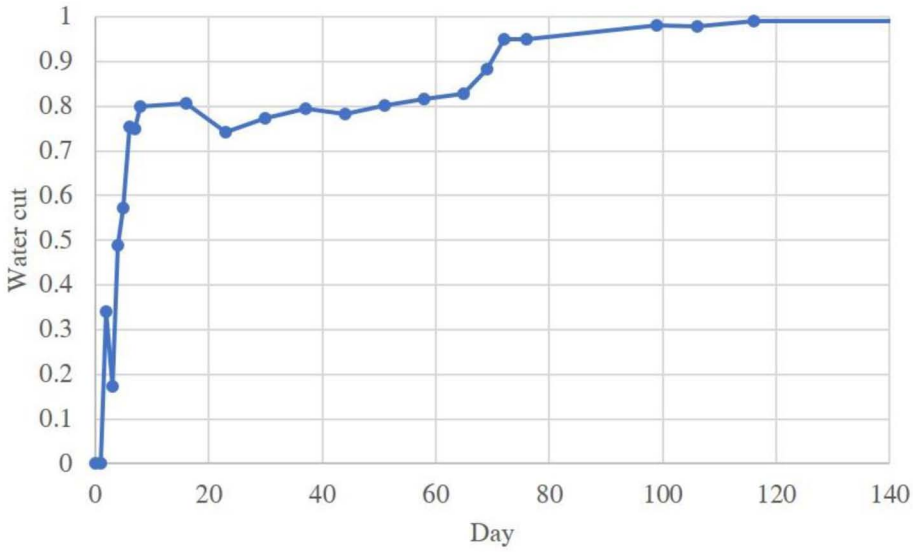

Figure 13—Water-cut response after CO_2 huff-n-puff in Well 271 by Simpson (1988)

Reasons for high-water cut

Initial water saturation. First, we assumed there were errors in the initial water saturation, and hence raised the initial water saturation Swi of each layer by 10%. One was used, if the new initial water saturation of a layer exceeded one. The new water-cut showed approximately a translation of 0.1 in vertical axis based on the previous curve as shown in Figure 14. But the trend still could not match the field observation. Initial water saturation though could significantly shift the water-cut might not be a reason behind above-mentioned abnormal water-cut behaviors after huff-n-puff.

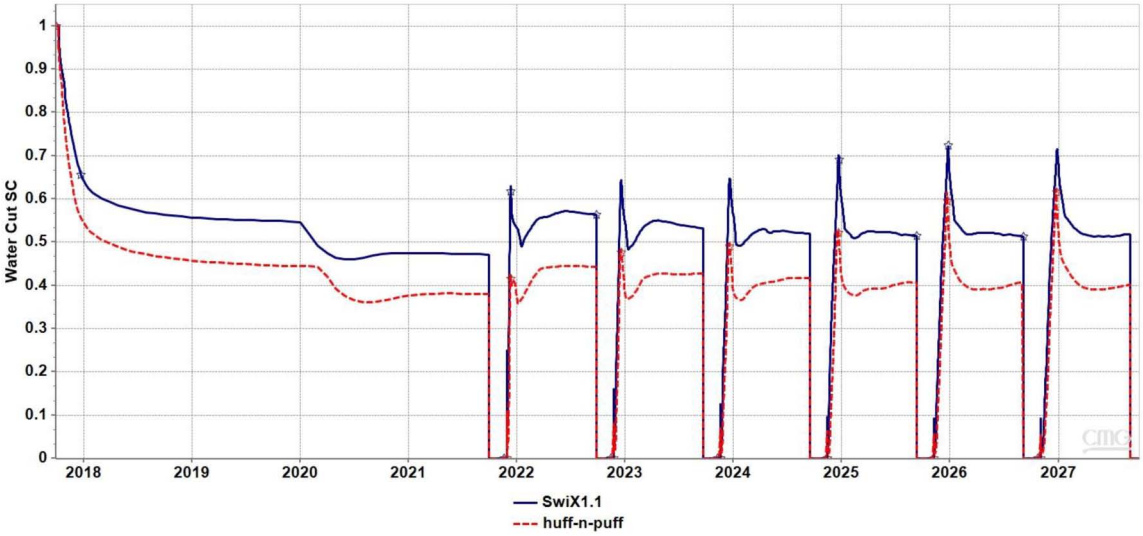

Figure 14—Water-cut after increasing the Swi

IFT-dependent relative permeability. By default, the CMG simulator would not consider the effect of interfacial tension on relative permeability (CMG, 2018) though it is a very important mechanism for miscible injection, which is the case in this study. We hence turned on the IFT-dependent relative permeability option. The new water-cut curve showed a decreased value of its peak, but an increased plateau value as shown in Figure 15. But overall, the oil recovery factor was almost unchanged with or without considering the IFT-dependent relative permeability. The reason might be that only oil and gas phase relative permeability are treated as function of IFT but not water relative permeability. However, according to Monger and Coma (1988), water-cut did increase from 0.30 to 0.67 after CO_2 injection above MMP. In this study, since MMP for CO_2 is 2020 psi based on our calculation, miscible injection is also the case for this pilot. Hence more related work on IFT-dependent water relative permeability might be required to further correlate MMP with high water-cut.

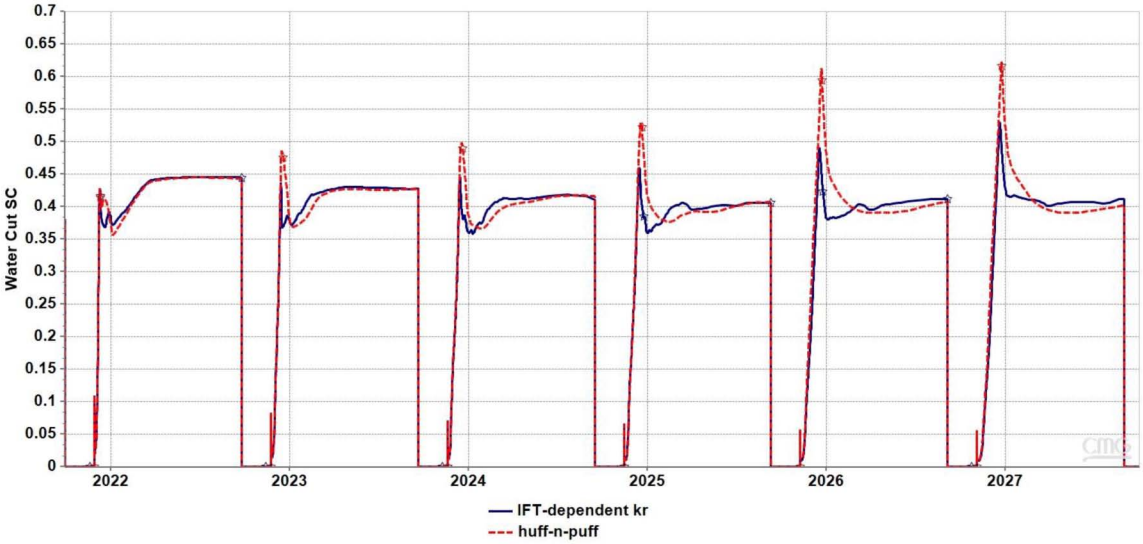

Figure 15—Water-cut after considering IFT-dependent relative permeability

Reopening of water bearing layers. Then we simulated the reopening of water bearing layers i.e. layer 9 and 12 by increasing the permeability of NF grid blocks from 0.025 mD to 0.25 mD, supposing that natural

fracture in these layers were reactivated due to gas injection. As shown in Figure 16, the water cut did increase, but the peak value was still lower than observed from the field.

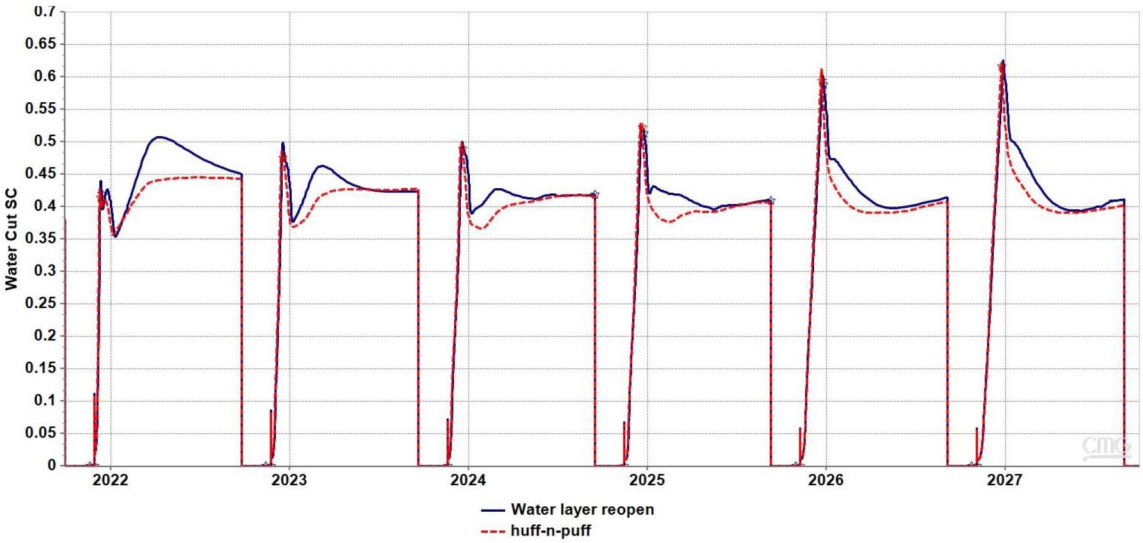

Figure 16—Water-cut considering reactivation of NF in layer 9, 10, 11 and 12

Reopening of unpropped hydraulic fractures. Previous studies by (Chen et al., 2015; Ishida et al., 2016) have shown the average breakdown pressure of supercritical CO_2 is only 73% of water due to its lower viscosity. The injected CO_2 in our case was in supercritical state under the injection pressure and in-situ temperature, and its breakdown pressure might be even lower with pre-existing hydraulic fractures. The reopening of fractures during huff-n-puff can also be verified to some extent by the CO_2 breakthrough observed in the pilot. CO_2 breakthrough was observed in offset wells at late time of injection under higher injection pressure, and its level would return to normal once the injection stopped. Moreover, the severity of breakthrough could be reduced by increasing injection pressure in a stepwise manner, which strongly indicates such inter-well connectivity is mostly dominated by the reopening of existing fractures. Hence, we hypothetically changed the relative permeability curve of unpropped fractures from matrix types, as shown in Figure 5 to fracture types, as shown in Figure 6, assuming that unpropped hydraulic fractures were reopened due to the injection of CO_2. Finally, we were able to obtain a relatively good match with field observations. As shown in Figure 17, the water-cut did increase due to enhanced fractional flow of water, and the water cut reached a maximum as 0.63. The water-cut slightly decreased with more cycles, but its value was still higher than the depletion value as 0.38 which is closer to the field observations. Figure 18 exhibits the different recovery factors among depletion, huff-n-puff base and huff-n-puff with high water-cut. And excessive water production would reduce the RF from 11.46% to 10.12%.

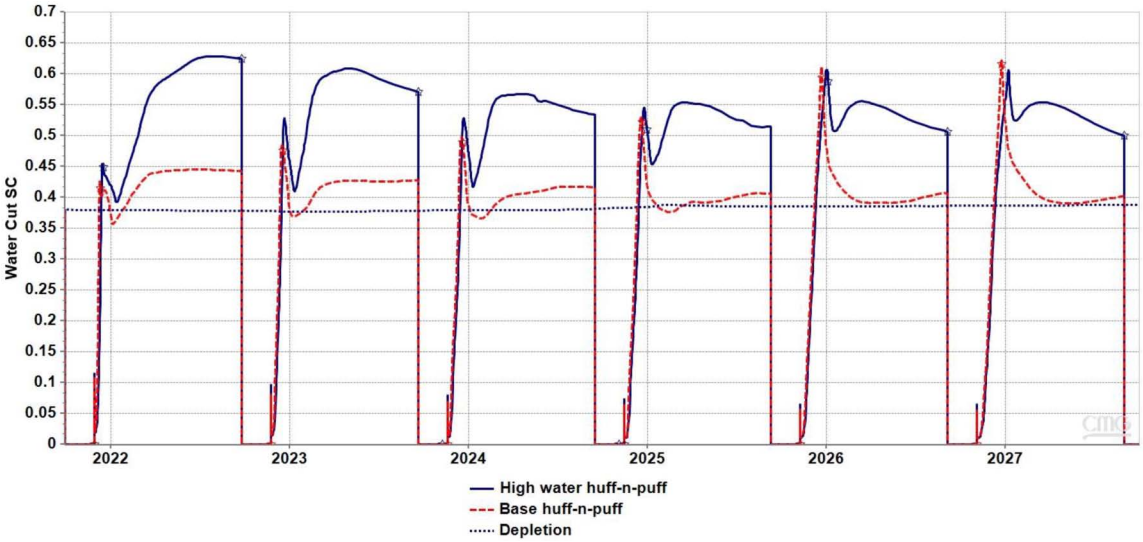

Figure 17—Water-cut considering reactivation of unpropped HF

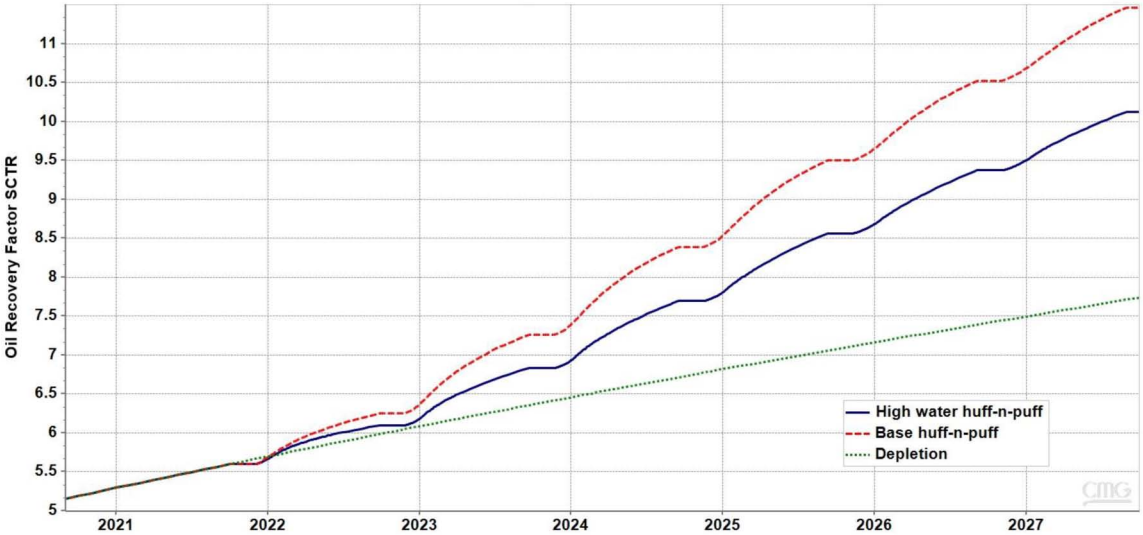

Figure 18—Comparison of recovery factors among cases

According to our simulation results, the most possible reason behind high water-cut is the reopening of unpropped hydraulic fracture. Hence, several operational constraints are proposed for the future work. For example, the maximum BHP must be tightly controlled at a lower value so as to restrain the unpropped hydraulic fracture from reopening when injecting CO_2 into the well. In addition, reactivation of water layers is one of the indispensable factors in processing high water-cut, and it could be controlled by BHP in this way as well. Other possible operational scheme will also be studied in the future work. Cyclic injection of hydrocarbon gas is being tested in other pilots. It will be investigated as well and then compared the results with CO_2 in the future. Moreover, we plan to utilize an in-house simulator to explore other possible reasons behind the water-cut rise, including wettability alteration, and chemical reactions between CO_2 and formation minerals, etc.

Summary

1. A recent huff-n-puff pilot in the Wolfcamp shale confirmed the effectiveness of CO_2 injection, meanwhile it witnessed higher than expected water-cut response in the puff stage. To understand the abnormal response,

a compositional modeling approach was implemented. Eight pseudo-components were lumped, and their thermodynamic properties were tuned to match the PVT experiment results using Peng-Robinson EOS. A lab-scale simulation model was first established to match the data from core experiment by adjusting relative permeability and rock compressibility.

2. A half stage model consisting of five fractures was established to represent a typical horizontal producer in this region. Oil RF was improved from 7.74% of depletion to 11.46% after six cycles of CO_2 huff-n-puff.

3. Several influencing factors on water-cut were simulated and identified including underestimation of initial water saturation, IFT-dependent relative permeability, reactivation of water-bearing layers, and re-opening of unpropped hydraulic fractures.

4. Field observed water-cut behavior was qualitatively matched in the simulation by shifting unpropped HF relative permeability curves from matrix-type to fracture-type after CO_2 injection. And excessive water production would reduce the RF to 10.12% when compared to a RF of 11.46% of huff-n-puff base case, which demonstrates the importance of water-cut management.

Acknowledgements

The authors would like to thank Energi Simulation for supporting this work. Computer Modelling Group is acknowledged for the software license.

Reference

Abethni, A. and Torabi, F., 2014. Oil recovery performance of immiscible and miscible CO_2 huff-and-puff processes. *Energy & Fuels*, **28** (2), pp.774–784.

Brown, M., Ozkan, E., Raghavan, R. and Kazemi, H., 2011. Practical solutions for pressure-transient responses of fractured horizontal wells in unconventional shale reservoirs. *SPE Reservoir Evaluation & Engineering*, **14** (06), pp.663–676.

Chen, Y., Nagaya, Y. and Ishida, T., 2015. Observations of fractures induced by hydraulic fracturing in anisotropic granite. *Rock Mechanics and Rock Engineering*, **48** (4), pp. 1455–1461.

CMG. 2018. GEM User's Guide. Computer Modeling Group.

Darvish, G. R., Lindeberg, E., Holt, T. and Utne, S.A., 2006. Laboratory experiments of tertiary CO_2 injection into a fractured core. *Paper SPE, 99649*, pp. 22–26.

Denoyelle, L. C. and Lemonnier, P., 1987, January. Simulation of CO_2 Huff n'Puff Using Relative Permeability Hysteresis. In SPE Annual Technical Conference and Exhibition. *Society of Petroleum Engineers*.

Energy Information Administration, 2019. Annual Energy Outlook 2019. U.S.

Haskin, H.K. and Alston, R.B., 1989. An evaluation of CO_2 huff 'n' puff tests in Texas. Journal of petroleum technology, **41** (02), pp. 177-184.

Hoffman, B.T., 2018, March. Huff-N-Puff gas injection pilot projects in the eagle ford. In SPE Canada Unconventional Resources Conference. *Society of Petroleum Engineers*.

Hsu, H.H. and Brugman, R. J., 1986, January. CO_2 huff-puff simulation using a compositional reservoir simulator. In SPE Annual Technical Conference and Exhibition. *Society of Petroleum Engineers*.

Ishida, T., Chen, Y., Bennour, Z., Yamashita, H., Inui, S., Nagaya, Y., Naoi, M., Chen, Q., Nakayama, Y. and Nagano, Y., 2016. Features of CO_2 fracturing deduced from acoustic emission and microscopy in laboratory experiments. *Journal of Geophysical Research: Solid Earth*, **121** (11), pp. 8080–8098.

Jin, L., Hawthorne, S., Sorensen, J., Pekot, L., Bosshart, N., Gorecki, C., Steadman, E. and Harju, J., 2017, April. Utilization of produced gas for improved oil recovery and reduced emissions from the Bakken Formation. In SPE Health, Safety, Security, Environment, & Social Responsibility Conference-North America. *Society of Petroleum Engineers*.

Pettit, J., and Muirhea, M., 2016, Permian Basin technical issues: (Part 1) How to manage water cut, https://ihsmarkit.com/research-analysis/permian-basin-technical-issues-part-1-how-to-manage-water-cut.html (accessed 4 May 2019).

Lai, S.Z. and Wardlaw, N.C., 1999. Factors Affecting the Application of Anti-Water Coning Technology (AWACT) At the South Jenner Oil Field, Southeast Alberta. *Journal of Canadian Petroleum Technology*, **38** (03).

Li, L., Sheng J. J., Su, Y. and Zhan, S., 2018. Further Investigation of Effects of Injection Pressure and Imbibition Water on CO_2 Huff-n-Puff Performance in Liquid-Rich Shale Reservoirs. *Energy & fuels*, **32** (5), pp. 5789–5798.

Luhning, R.W., Chmilar, M.J. and Anderson, B.S., 1990, January. The AOSTRA Anti Water Coning Technology (AWACT) Process-From Invention to Commercial Application. In Annual Technical Meeting. *Petroleum Society of Canada*.

Mohammed, S.L., Singhal, A.K. and Sim, S., 2006. Screening criteria for CO_2 huff-n-puff operations. SPE 100044.
Monger, T.G. and Coma, J.M., 1988. A laboratory and field evaluation of the CO_2 huff n'puff process for light-oil recovery. SPE reservoir engineering, **3** (04), pp. 1-168.

Monger, T.G., Ramos, J.C. and Thomas, J., 1991. Light oil recovery from cyclic CO_2 injection: influence of low pressures impure CO_2, and reservoir gas. *SPE Reservoir Engineering*, **6** (01), pp. 25–32.

Pankaj, P., Mukisa, H., Solovyeva, I. and Xue, H., 2018, Enhanced oil recovery in eagle ford: opportunities using huff-n-puff technique in unconventional reservoirs. In SPE Liquids-Rich Basins Conference-North America. *Society of Petroleum Engineers*.

Sheng, J.J., 2015. Enhanced oil recovery in shale reservoirs by gas injection. *Journal of Natural Gas Science and Engineering*, **22**, pp. 252–259.

Simpson, M.R., 1988. The CO_2 huff and puff process in a bottomwater-drive reservoir. *Journal of petroleum technology*, **40** (07), pp. 887–893.

Song, C. and Yang, D., 2017. Experimental and numerical evaluation of CO_2 huff-n-puff processes in Bakken formation. *Fuel*, **190**, pp. 145–162.

Todd, H.B. and Evans, J.G., 2016, May. Improved oil recovery IOR pilot projects in the Bakken formation. In SPE Low Perm Symposium. *Society of Petroleum Engineers*.

Torabi, F. and Asghari, K., 2010. Effect of operating pressure, matrix permeability and connate water saturation on performance of CO_2 huff-and-puff process in matrix-fracture experimental model. *Fuel*, **89** (10), pp. 2985–2990.

Tovar, F.D., Eide, O., Graue, A. and Schechter, D. S., 2014, April. Experimental investigation of enhanced recovery in unconventional liquid reservoirs using CO_2: a look ahead to the future of unconventional EOR. In SPE Unconventional Resources Conference. *Society of Petroleum Engineers*.

Tian, Y., Xiong, Y., Wang, L., Lei, Z., Zhang, Y., Yin, X. and Wu, Y. S., 2019, March. A Compositional Model for Gas Injection IOR/EOR in Tight Oil Reservoirs Under Coupled Nanopore Confinement and Geomechanics Effects. In SPE Reservoir Simulation Conference. *Society of Petroleum Engineers*.

Wang, L., Tian, Y., Yu, X., Wang, C., Yao, B., Wang, S., Winterfeld, P.H., Wang, X., Yang, Z., Wang, Y. and Cui, J., 2017. Advances in improved/enhanced oil recovery technologies for tight and shale reservoirs. *Fuel*, **210**, pp. 425–445.

Yang, J., Wang, X., Peng, X., Du, Z. and Zeng, F., 2019. Experimental studies on CO_2 foam performance in the tight cores. *Journal of Petroleum Science and Engineering*, **175**, pp. 1136–1149.